International Journal of Mechanical Engineering (IJME)
ISSN (P): 2319-2240; ISSN (E): 2319-2259
Vol. 6, Issue 4, Jun - Jul 2017; 1-14

International Academy of Science, Engineering and Technology
Connecting Researchers; Nurturing Innovations

MODELING AND PERFORMANCE EVALUATION OF AN INDIRECT SOLAR DESALINATION SYSTEM

K.K.MATRAWY

Department Mechanical Engineering, Assiut University, Assiut, Egypt

ABSTRACT

The present study is concerned about a mathematical model developed, to study the performance of a truncated cone solar heater (TCSH), connected by a multi effect still (MES). The proposed TCSH included: a glass cover, truncated cone reflector, and a blackened vessel. The truncated cone shape is used as a reflector without a continuous tracking, where one half is always facing to the sun for the whole day hours. The effective area of the glass cover through which, the transmitted radiation is reflected to the vessel, derived as a function of the solar incidence angle and the geometry of the conical surface. The ratio of the vessel radius of the glass cover one is studied as a design parameter. The final results showed that an acceptable productivity from the MES with a maximum value of 0.97 kg/hr-m^2 at noon times can be obtained. Also, the productivity of MES decreases by about 38 % as the ratio of vessel radius to the cover one increases by three times.

KEYWORDS: Truncated Cone Solar Heater, Multi Effect Still, Effective Area, Productivity

Nomenclature		Greek Letters		Subscripts	
A	area (m^2)	α	angle in Fig. (A2), absorptivity (-)	*1,2*	left and right half of the conical surface
C_p	specific heat (J/m k)	β	expansion coefficient (°)	*a*	air
h	Heat Transfer Coefficient (W/m^2 K)	β_i	Angle in Fig. (A2)	*abs*	absorbed
H	height (m)	γ	surface azimuth angle (°)	*amb*	ambient
I	solar radiation (W/m^2)	γ_i	angle in Fig. (A2)	*b*	brine
L	distance (m)	ϕ	latitude angle (°)	*c*	cover, convection
m	mass (kg)	ω	solar hour angle (°)	*cs*	conical surface
t	time (s), thickness (m)	δ	solar declination angle (°)	*d*	distillate
T	temperature (°C)	θ_i	solar incident angle (°)	*e*	evaporation
S	slope angle (°)	ρ	density (kg/m^3), reflectivity(-)	*eff*	effective
R	radius (m)	τ	transitivity (-)	*i*	surface i
Q	heat (W)			*j*	surface j
X	distance (m)			*L*	losses
				Lat	latent
				h	horizontal
				v	vessel
				vc	vessel cover
				vs	vessel surface
				r	radiative, reflected
				s	stage, surface

INTRODUCTION

Simple basin solar still has a lower productivity, which is referred to the dissipation of the latent heat of condensation as a wasted energy. One option to enhance the productivity is introducing the multi effect still. Many studies were developed for the multi effect solar still [1-5]. The effect of number of stages on the daily productivity is studied by Al Mahdi [6]. The results show that the double stages still give the highest efficiency, while the triple and quadruple stages improved the productivity by an appreciable value during the night. The study showed that an increase of the number of

basins beyond four stages has not increased the productivity significantly. Double basin solar still is examined for various systems and weather conditions, where its productivity increases by 36 % than the single basin one [7]. Also, the productivity can be enhanced by decreasing the glass cover temperature using continuous flow [8] or intermittent flow [9], but it will dissipate the latent heat of condensation. Tiwari et al [10] concluded that the total productivity of the double basin solar still is, strongly depended on the water depth in the lower basin. For less water depth, the yield was enhanced, but the distillation decreases during the night times. For greater water depth, the distillation output is reduced, but distillation continues even during the night. An inverted absorber double basin solar still is proposed and tested by [11 and 12]. In this design, the water temperature can be increased by inverting the absorber which reduces the bottom heat losses. A double basin solar still is studied by Tiwari [13] using water flow over the glass cover and at the same time a flat plate collector supplied hot water in the lower basin. The study showed that using the flat plate collector could increase the productivity by about 50 % than the normal double basin still. The flat plate collector can be used with a theromosyphon circulation or forced one [14]. Badran et al. [15] integrated flat plate collector with a conventional type solar still where the yield increases by 52 % due to the coupling of the flat plate collector. Some improvements have been developed for the flat plate collector connected with the solar still such as using a double rectangular enclosure where the top enclosure is filled with paraffin wax while the bottom one is with water [16]. Also, the improvement included using of an aluminum-water nano-fluid [17] enhancing the efficiency up to 85.63 % by adding suspended aluminum nano-particles into pure water. Compound parabolic concentrator with forced circulation coupled to a double basin solar still is suggested in [18]. The results showed that a decrease of the productivity occurred due to decrease of the difference between water and glass temperatures. However, the productivity, improved due to utilization of latent heat of condensation. Moreover, a heat exchanger inside the lower basin of multi effect still is suggested and studied in [19]. The author observed that the efficiency of the still with heat exchange is less than that without a heat exchanger. Also, the study showed that the efficiency, enhanced by the increase of the mass flow rate in the range of 0-20 kg/hr and by increasing the length of the heat exchanger pipe in the range of 0-5m. A transient model for multi stage evacuated solar desalination system is developed in [20]. It was found that the optimum configuration for four stages satisfied with a 10mm gap between the stages and mass flow rate of 55 kg/m^2/day. The thermal performance and economic feasibility of a single and double basin solar still is studied in [21]. The results showed that the optimum mass of the brine in the lower basin was about 20 kg/m^2.

PLAN AND DESCRIPTION OF THE PROPOSED SYSTEM

Based on the previous works of multi effect solar still, it can be concluded that the using of one or more glass covers as a condensing surface may constrain the number of stages. Also, the transmission of radiation through the glass cover may increase the cover temperature and consequently decreases the productivity. In addition, coupling solar concentrators by the solar still needed a continuous tracking which may increase the cost of the system. Thus, in the present study, it is proposed to use a number of aluminum trays as condensing surfaces by which the glass covers are eliminated. On the other hand, a primary design of the truncated cone surface as a solar cooker is suggested and tested experimentally by the author [22]. But there are no modeling or simulation results developed by the author or other ones up to the present time in order to cover the topic and to study the design and performance parameters. Also, the experimental study was limited only for a short period (1-1.5 hrs) at noon times where there is a normal incidence without any details or information at morning and late afternoon times. Thus, these reasons encourage the author to develop a mathematical model for the truncated cone shape as a solar heater connected by four stages still in the present study. A schematic diagram for the proposed system is shown in Figure (1).

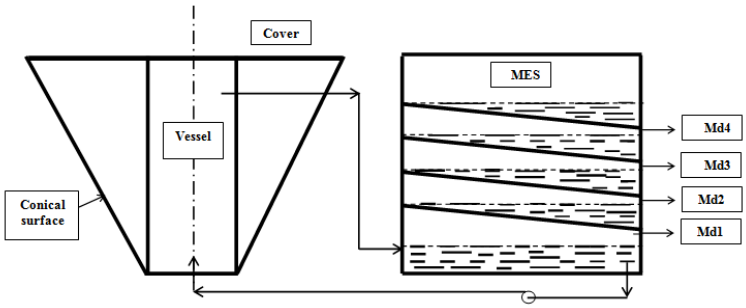

Figure 1: A Schematic Diagram for the Truncated Cone Solar Heater Connected by Four Stages Still

The main components of the proposed TCSH are:

1. Stainless steel conical surface with a thickness of 1mm used as a reflector for the transmitted radiation through the glass cover.
2. Glass cover with a thickness of 6 mm white glass.
3. Blackened heating vessel with a radius of R_1 = 0.05 - 0.15 m and a height calculated based on the given radius.
4. Outer frame from galvanized steel with a gap of 5cm filled with polyurethane foam to decrease the heat losses and protects the heater from the environmental risks.

For the multi effects still, it consists of a number of aluminum trays arranged in a way to allow the condensation on the lower surface while an amount of water put on the other side. The latent heat of condensation for the main basin as a first stage is used for the second one. At the same time, this procedure is repeated for the following stages up to the final stage at the top of the unit.

MATHEMATICAL MODEL

The developed model is based on an energy balance for various components to obtain the productivity produced by the proposed system. The model included sub-models for truncated cone heater and also multi effects still. The developed model is detailed in the following sub-sections followed by the determination of the various heat transfer coefficients.

Modeling of the Truncated Cone Solar Heater

The heat transfers exchanged between the different components of the (TCSH) are shown in Figure. (2).

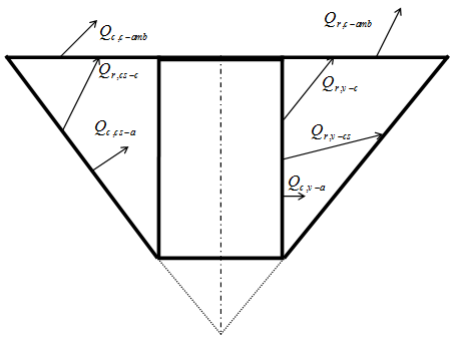

Figure 2: Energies Exchange between the Components of TCSH

The energy balance equations concerning by the conical surface, vessel, glass cover, and inside air are given in Eqs (1-4), respectively, as:

$$\left(mC_p\right)_{cs}\frac{dT_{cs}}{dt}=Q_{s,cs}+Q_{r,v-cs}-Q_{r,cs-c}-Q_{c,cs-a}-Q_{L,cs} \quad (1)$$

$$\left(mC_p\right)_{v}\frac{dT_{v}}{dt}=Q_{s,v}-Q_{r,v-cs}-Q_{r,v-c}-Q_{c,v-a}-Q_{mes} \quad (2)$$

$$\left(mC_p\right)_{c}\frac{dT_{c}}{dt}=Q_{s,c}+Q_{r,cs-c}+Q_{r,v-c}-Q_{c,c-a}-Q_{r,c-amb}-Q_{c,c-amb} \quad (3)$$

$$\left(mC_p\right)_{a}\frac{dT_{a}}{dt}=Q_{c,cs-a}+Q_{c,v-a}+Q_{c,c-a} \quad (4)$$

The determinations of the absorbed radiations, $Q_{s,i}$ through the i^{th} component of the (TCSH) are derived in Appendix (A). The radiative, convective heat transfers in Eqs (1-4) between two surfaces i and j are expressed as a function of the heat transfer coefficients by:

$$Q_{r,i-j}=A_i h_{r,i-j}\left(T_i-T_j\right) \quad (5)$$

$$Q_{c,i-j}=A_i h_{c,i-j}\left(T_i-T_j\right) \quad (6)$$

While the heat transfer, exchange between the (TCSH) and (MES) in Eq. (2) is given by:

$$Q_{mes}=m_b C_{p,b}\left(T_v-T_{s1}\right) \quad (7)$$

Where: m_b is the mass flow rate of the brine circulated between the vessel and MES and T_{s1} is the uniform temperature of the first stage in the basin. The ambient air temperature equation used in the calculations is based on the maximum and minimum values for the month and is detailed in Ref. [23].

Modeling of Multi Effect Still

The multi effect still included four stages with temperatures ranged from T_{s1} up to T_{s4}. The proposed still is shown in Figure. (3).

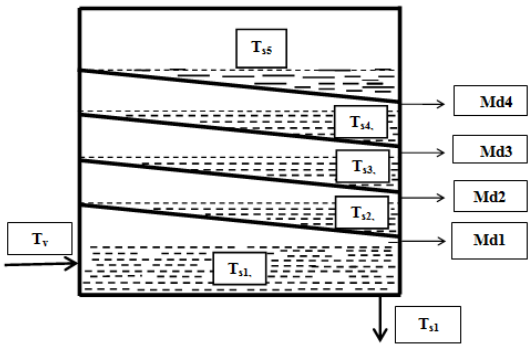

Figure 3: An Energy Balance between the Stages of MES

An energy balance for the *1st* stage yields:

$$\left(mC_p\right)_{s1}\frac{dT_{s1}}{dt}=m_b^{\cdot}C_{p,b}\left(T_v-T_{s1}\right)-Q_{c,s1\to s2}-Q_{e,s1\to s2}-Q_{r,s1\to s2}-Q_{L,s1} \quad \textbf{(8)}$$

For the *2nd* and *3rd* stages, the energy balance is:

$$\left(mC_p\right)_{s,i}\frac{dT_{s,i}}{dt}=Q_{lat,s(i-1)\to si}-Q_{c,si\to s,i+1}-Q_{e,si\to s,i+1}-Q_{r,si\to s,i+1}-Q_{L,si} \quad \textbf{(9)}$$

While for the *4th* stage:

$$\left(mC_p\right)_{s4}\frac{dT_{s,4}}{dt}=Q_{lat,s3-s4}-Q_{c,s4-s5}-Q_{e,s4-s5}-Q_{r,s4-s5}-Q_{L,s4} \quad \textbf{(10)}$$

Where the quantity: Q_{lat} is the latent heat of condensation, while the Q_c, Q_e and Q_r are the convective, evaporative and radiative heat transfers, respectively. Their values are given by:

$$Q_{c,si\to s(i+1)}=A_{si}\ h_{c,si\to s(i+1)}\left(T_{si}-T_{s(i+1)}\right) \quad \textbf{(11)}$$

$$Q_{e,si\to s(i+1)}=A_{si}\ h_{e,si\to s(i+1)}\left(T_{si}-T_{s(i+1)}\right) \quad \textbf{(12)}$$

$$Q_{r,si\to s(i+1)}=A_{si}\ h_{r,si\to s(i+1)}\left(T_{si}-T_{s(i+1)}\right) \quad \textbf{(13)}$$

The values of h_c, h_e, h_r are given in detailed in sub-section.

Finally, the output productivity from the i^{th} stage is given by:

$$m_{d,i}=\frac{Q_{e,si}}{Q_{lat,si}} \quad \textbf{(14)}$$

Which gives the total productivity $m_{d,t}$ by:

$$m_{d,t}=\sum_{i=1}^{i=4}m_{d,i} \quad \textbf{(15)}$$

Heat Transfer Coefficients

For the TCSH: The heat transfer coefficient between the vessel as a vertical plate and inside air is given by [24 and 25]:

$$Nu_L=\left\{0.825+\frac{0.387Ra_L^{1/6}}{\left[1.0+(0.492/\mathrm{Pr})^{9/16}\right]^{8/27}}\right\}^2 \quad \textbf{(16)}$$

The heat transfer coefficient between the glass cover and inside air is given by [25]:

$$Nu_L=0.54\,Ra_L^{1/4} \qquad \text{for } 10^4\le \mathrm{Ra_L}\le 10^7 \quad \textbf{(17)}$$

$$Nu_L = 0.15\,Ra_L^{1/3} \quad \text{for } 10^7 \le \text{Ra}_\text{L} \le 10^{11} \tag{18}$$

$$Ra_L = \frac{g\,\beta(T_s - T_a)L^3}{\alpha\upsilon} \tag{19}$$

Where, the convective heat transfer coefficient between the conical surface and inside air is calculated by Eqs. (17-19) replace g by g cos α, where the conical surface can be divided into a number of segments each with a slope angle α.

For the MES: the convective and evaporative heat transfer coefficients are given in Ref. [26].

The radiative heat transfer coefficients for TCSH and MES are given by [26] as:

$$h_{r,i-j} = \frac{\sigma(T_i + T_j)(T_i^2 + T_j^2)}{\frac{1-\varepsilon_i}{A_i\varepsilon_i} + \frac{1}{A_i F_{i-j}} + \frac{1-\varepsilon_j}{A_j\varepsilon_j}} \tag{20}$$

Where, the view factor F_{i-j} depends on the configuration of the surface *I* compared to the surface *j*. The value of F_{i-j} is detailed in Ref. [25 and 27].

RESULTS AND DISCUSSIONS

The simulation results for the various variables concerning by the TCSH and also the MES will be presented and discussed in the present section. The presented results are based on the following data (referred to Figure A1) are: R_1 = 0.05 m, R_2 = 0.5 m, α = 45°, H = 0.45 m, t_c = 6 mm (white glass), t_{CS} = 1 mm, α_v = 0.9, α_{cs} = 0.1, α_c = 0.1.

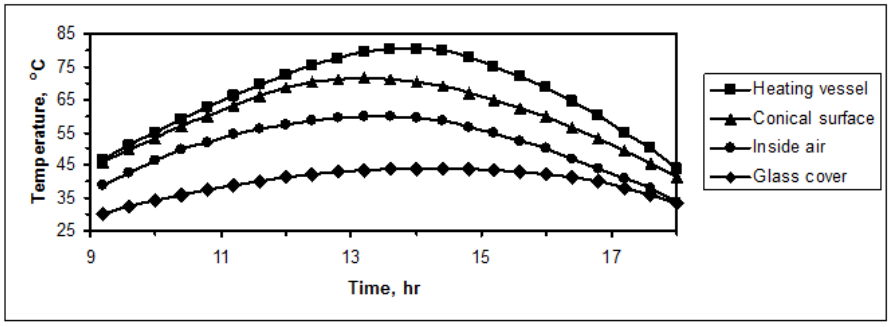

Figure 4: Different Temperatures versus Day Hours of the Truncated Cone Solar Heater

The temperatures of different components of TCSH including the heating vessel, conical surface, inside air beside the glass cover are shown in Figure. (4). It can be seen that the highest temperature is achieved with the heating vessel due to the absorbed radiation reflected from the conical surface in addition to the absorbed radiation transmitted to the vertical surface and cover of the vessel. It is important to note that the reflected radiation from the conical surface to be absorbed through the vessel is maximized at normal incidence due to the half cone angle of 45° which directed the reflected radiation horizontally. Maximum temperature for the vessel has a value of about 81 °C through the period 13:30 -14 p.m. The temperature of the conical surface is lower than that for the vessel as seen in the figure. Then, the inside air temperature is the lowest one than the vessel and conical surface temperatures. Maximum values of 71 °C and 59 °C are attained for the conical surface and inside air, respectively. Glass cover temperature has the minimum temperature in the

TCSH. The lower temperature of the glass cover is mainly referred to its lower absorptivity beside the slight stored energy due to the small difference of the heat exchanges between the top and lower sides of the cover.

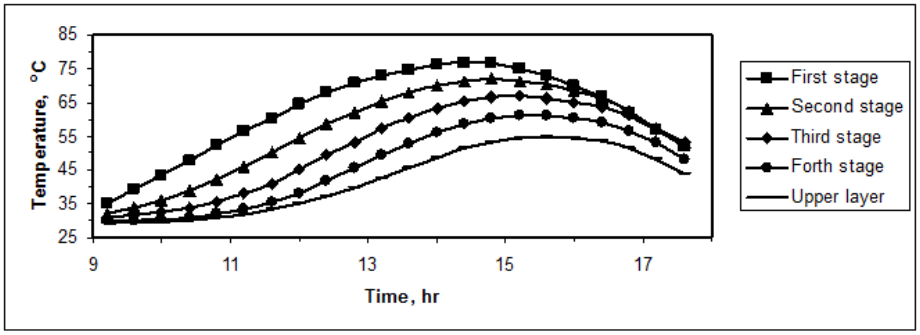

Figure 5: Different Temperatures of the Multi Effect Still Versus Day Hours

Figure (5) shows the stages temperatures of multi-effect still versus the day hours. Lower stage or basin of the MES has the highest temperature, then, the temperatures of the next stages decrease as the number of stages increases, i.e. $Ts_1 \geq Ts_2 \geq Ts_3 \geq Ts_4 \geq Ts_5$ as seen in the figure. Maximum temperature for the MES occurred with lower basin with a value of about 77 ^{o}C. At the same time, the maximum temperature difference between the first and second stages is nearly 8-9 oC,which decreases with the increase of the stage number. At the day's end, it nearly approached for the whole temperatures, which is referred to the relaxation case for the system due to the decrease or absence of the incident's solar radiation.

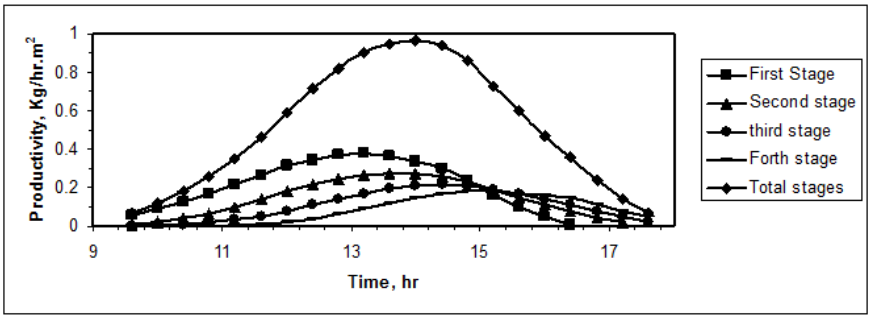

Figure 6: Productivities versus Day Hours for Different Stages of Multi Effect Still

Hourly productivities, out by MES versus day hours are presented in Figure (6). The presented productivities are presented for each stage versus day hours. The total productivity is the summation of the whole ones. From the given figure, it can be seen that the lower stage satisfies the highest productivity with a maximum value of 0.38 kg/hr-m^2 which may be referred to the higher input energy. Under these conditions, the total productivity was about 0.97 kg/hr-m^2 as seen in the figure. This means that the first stage can contribute by about 39 % of the total productivity. For the other stages, the maximum productivities were not satisfied at the same time and their values are: 0.27, 0.21 and 0.16 kg/hr-m^2 for the second, third and forth stages, respectively. This means that the different contributions for different stages are: 27%, 21% and 16% for the second, third and fourth stages respectively, which confirmed the results developed in Ref. [6] and increasing the number of stages more than four stages may not contribute by a significant value. Also, the trends of the different stages productivities of MES may be enforced at late time after noon. This may be related to the relaxation state of the first stage due to the decrease of the solar radiation incident on the TCSH while there is an activity of condensation occurred in the other stages. As an example, at 16 p.m., the maximum productivity occurred by about 0.15 kg/hr-m^2 at the

3rd and 4th stages while the minimum one occurred with the 1st stage with value of 0.05 kg/hr.m^2 as seen in the figure. On the other hand, the summation of the stages productivities gives the total productivity for the MES which is presented on the same figure with a maximum value of about 0.97 kg/hr-m^2 at about 14 p.m as seen in the figure.

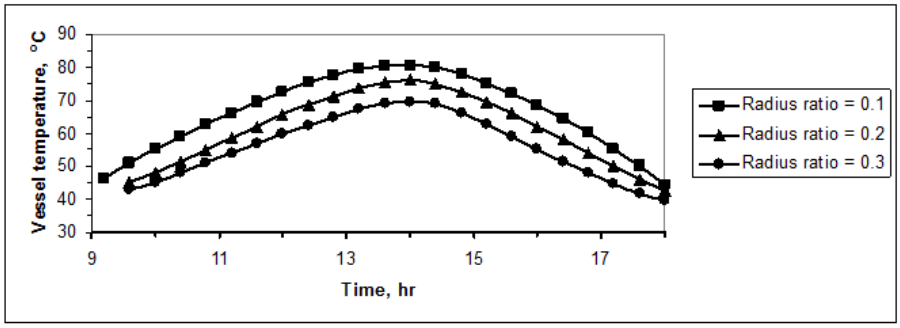

Figure 7: Vessel Temperature versus Day Hours at Different Radius Ratios

One important design parameter which affects the performance of the TCSH and consequently the productivity of MES is, the radius ratio (i.e. ratio of the vessel radius to the glass cover radius). The previous results in Figure (4-6) are presented at radius ratio: R_1/R_2 = 0.05/0.5=0.1. In the next case, the simulation results are presented at radius ratio of 0.2, and 0.3 and compare by the ratio of 0.1. This selection may cover the most applied range for the dimensions of the vessel and glass cover. Other dimension for TCSH and MES are the same.

Figure (7) shows the heating vessel temperature versus day hours at different radius ratios. It is clear from the figure that the vessel temperature increases significantly as the radius ratio decreases. The maximum vessel temperature for the ratio of 0.1 has a value of 81 ^{o}C while, the corresponding values with the ratio of 0.3 is 70 ^{o}C at the same hour. For the case of ratio 0.2, its temperature is in between. The interoperation of the increase of the vessel temperature as the radius ratio decreases is referring to the increase of the heat capacity of the fluid in the vessel accomplished the lower radius ratio. On the other hand, the vessel surface area increases with the increase of the radius ratio, but with a lower rate than that for the decrease of the heat capacity.

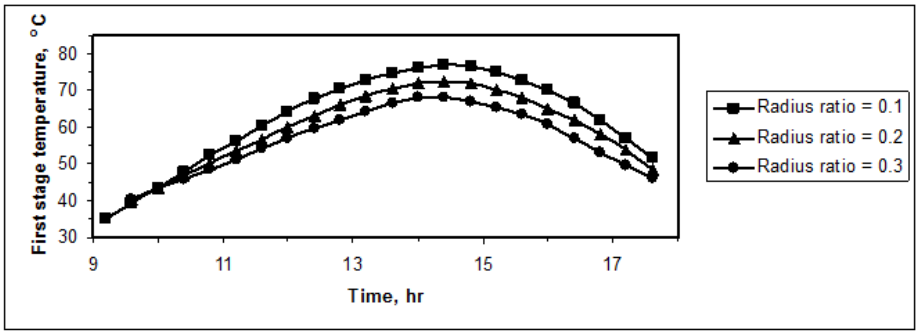

Figure 8: First Stage Temperatures versus Day Hours at Different Radius Ratios

Figure (8) shows the variation of the 1st stage temperature in MES versus day hours at different radius ratios. The temperature of the 1st stage is parallel to that with the heating vessel which means an increase with the decrease of R_1/R_2. Also, a difference of temperatures between the curves is about 5-6 ^{o}C can be observed at noon times. Maximum temperature of about 77 ^{o}C is observed at the ratio R_1/R_2=0.1, while the corresponding value is about 68 ^{o}C at R_1/R_2 = 0.3. These results show the importance and necessity to decrease the ratio R_1/R_2 through the design of TCSH.

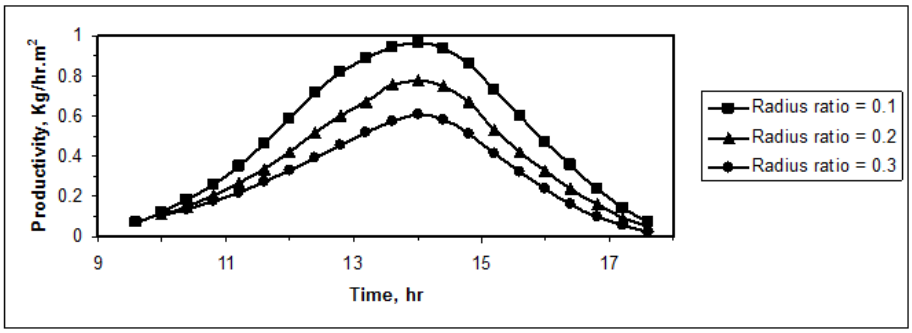

Figure 9: Productivity of Multi Effect Still Versus Day Hours at Different Radius Ratios

The productivity of the MES with different radius ratios R_1/R_2 is shown in Figure (9). Based on the presented results and discussions for Figure (7) and (8), it can be concluded the highest productivity occurred with the ratio of 0.1, while the lowest one with a ratio of 0.3. Maximum productivity of 0.97 kg/hr-m^2 is achieved at the ratio of 0.1, while the minimum one is about 0.61 kg/hr-m^2 with the ratio of 0.3. This means that the productivity of MES decreases by about 38 % as the radius ratio increases three times. The reasons for the high productivity at R_1/R_2 = 0.1 may be the same ones of the temperatures of the heating vessel and 1st stage as discussed previously.

CONCLUSIONS

Mathematical modeling of the solar truncated cone heater connected by four stages still, is developed through the present study. The developed model included a derivation of the effective area of the glass cover through which the reflected radiation is absorbed through the vessel, particularly at morning and after noon times. At noon times, all transmitted radiation is reflected horizontally and absorbed through the vessel when the half conical angle is 45^o. The vessel temperature has a higher value when the ratio of the vessel radius to the cover one is 0.1. As a result, the productivity of the connected four stages still is enhanced significantly with a maximum value of 0.97 Kg/hr-m^2 at noon times. Furthermore, using more than one stage i.e. four stages could contribute by about of 60 % from the total productivity of MES.

REFERENCES

1. Mahmoud I.M. Shatat and Mahkamov K. Determination of rational design parameters of multi stage solar water desalination still using transient mathematical model. Renewable Energy 2010: 35:52-61.
2. Prem Singh, Parmpal Singh, Japdeep Singh, and Krishnendu Kundu. Performance evaluation of low interia multi stage solar still. International Multi Conference of Engineering and Computer Science, Hong Kong, Vol. II. March 12-14, 2012.
3. Rasool Kalbasi and Mehdi Nasr. Multi passive desalination system, an experimental approach. World Applied Science J. 2010:10:1264-1271.
4. Ashivini Kumar and Adhikari R.S. Cost optimization studies on multi stage stacked tray solar still. Desalination 1999: 125:115-121.
5. Yousif A Abakr, Ahmed F. Ismail and Mirghani I. Ahmad. Parametric study of an evacuated multi stage solar still. ASME international solar energy conference, Portland, Oregon, USA, July 11-14, 2004.

6. Al Mahdi N. Performance prediction of a multi basin solar still. Energy 1992:17:87-93.

7. Sodha MS, Nayak IK, Tiwari GN, Kumar Ashvini. Double basin solar still. Energy Conversion and Management 1979:20: 23-32.

8. Abu-Hijleh BAK. Enhanced solar still performance using water film cooling of the glass cover. Desalination 1996: 107: 235-244.

9. Tiwari GN, Madhuri Garg HP. Effect of water flow over the glass cover of a single basin solar still with an intermittent flow of wasted hot water in the basin. Energy Conversion and Management 1985: 25:315-322.

10. Tiwari GN, Chetna S, Yadav YP. Effect of water depth on the transient performance of a double basin solar still. Energy Conversion and Management 1991:32:293-301.

11. Tiwari GN, Sangeeta S. Performance evaluation of an inverted absorber solar still. Energy Conversion and Management 1998: 39: 173-180.

12. Sangeeta S, Tiwari GN. The effect of depth on the performance of an inverted absorber double basin solar still. Energy Conversion and Management 1999:40:1885-1897.

13. Tiwari GN. Enhancement of daily yield in a double basin solar still. Energy Conversion and Management 1985: 25:49-50.

14. Yadav YP. Transient analysis of the double basin solar still integrated with collector. Desalination 1989: 71: 151-164.

15. Bbadran A., Ahmad A., Emad E.S., and Mahammad O. A solar still augmented with a flat plate collector. Desalination 2005: 172: 227-234.

16. Reddy S. Thermal modeling of PCM-based solar integrated collector-storage water heating system. Solar energy engineering 2007: 129:458-464.

17. Mustafa Turkyimazoglu. Performance of direct absorption solar collector with nano-fluid mixture. Energy conversion and management 2016: 114:1-10.

18. Bhagwan P., Tiwari GN. Analysis of double effect active solar distillation. Energy conversion and management 1996: 37:1647-1656.

19. Yadav YP. Performance analysis of a solar still coupled to a heat exchanger. Desalination 1993:91:135-144.

20. Vishwannath Kumar P., Ajay Kumar Kaviti, Om Prakash and Reddy K.S. Optimization of design and operating parameters on year round performance of multi stage evacuated solar desalination system using the transient model. Int. J. Energy and Environment 2012: 3:409-434.

21. Phillips O. Agboola, U. Atikol and Hossein Assefi. Feasibility assessment of basin solar stills. Int. j. Green Energy 2015:12:139-147.

22. Matrawy K.K. High efficiency solar cooker-comparative study with the conventional type. Bulletin of the Faculty of Engineering, Assiut University 2001:29:71-79.

23. Matrawy K.K., Mahrois A-F, and Youssef M.S. Energy management and parametric optimization of an integrated PV solar house. Energy conversion and management 2015: 96: 377-383.

24. Thulasi Das T.C., Karmak Ar S., and Rao D.P. Solar box cooker, Part 1- Modeling. Solar Energy 1994: 52: 265-272.

25. Theodore L. Bergman, Adrienne S. Lavine, Frank P. Incropera and David P. Dewitt. Fundamentals of heat and mass transfer, 7th ed., 2011, John Wiley & Sons.

26. Matrawy K.K., Alosaimy A.S., Mahrous A-F. Modeling and experimental study of a corrugated wick type solar still: comparative study with a simple basin type. Energy conversion and management 2015: 105: 1261-1268.

27. Rea S.N. Rapid method for determining concentric cylinder radiation view factors. AIAA Journal 1975: 133 (8):1121-1122.

28. Elsayed MM, Taha IS and Sabbagh JA. Design of solar thermal systems. 1st ed., Scientific Publications Center, King Abdulaziz University, Jeddah, 1994.

APPENDIX (A)

Absorbed Radiation through the Heating Vessel

The absorbed solar radiations through the components of the (TCSH) in Eqs (1-4), are derived based on the different paths of the radiation incident on the glass cover as shown in Figure (A1). For any hour through the day, the conical surface can be divided into a left half, which is always facing the sun beside the right one which received a little radiation due to its opposite orientation to the sun. If the conical surface is divided into N segments, it is possible to show that each segment has its own orientation, i.e. surface azimuth angle with respect to the south direction. Hence, for a given i^{th} segment the angle of incidence of transmitted radiation on the conical surface (i.e. $\theta_{1,i}$ or $\theta_{2,i}$) as shown in Figure (A1) can be given by the following expression as [28]:

$$\begin{aligned}\cos\theta_i &= (\cos s\,\sin\phi - \sin s\,\cos\phi\cos\gamma)\sin\delta \\ &+ (\cos s\,\cos\phi + \sin\phi\sin s\,\cos\gamma)\cos\delta\cos\omega \\ &+ \cos\delta\sin s\,\sin\gamma\sin\omega\end{aligned} \qquad \textbf{(A1)}$$

Figure (A1) showed for a one segment in the left half of the CS, the radiation incident on the cover at point **e**, transmitted through the cover and incident on the conical surface at point **b** with incidence angle θ_i. Then, it reflects and transmitted again through the cover at point **c** (Upper edge of the vessel). This means that all radiations reached the CS along the line ***ab*** is reflected and escape to the ambient. Hence, the effective area of the cover through which the reflected radiation is absorbed through the blackened vessel is represented by the line **ec** (see plan view of Figure A1).

The derivation of the effective area of glass cover for the i^{th} segment of the CS is based on the following geometrical relations for the triangles ***abc*** and ***abe*** as given in Figure (A2).

$$\beta_i = \pi - \alpha - (\frac{\pi}{2} - \theta_{1,i}) = \frac{\pi}{2} - \alpha + \theta_{1,i} \qquad \textbf{(A2)}$$

$$\gamma_i = \pi - \alpha - (\frac{\pi}{2} + \theta_{1,i}) = \frac{\pi}{2} - \alpha - \theta_{1,i} \quad \textbf{(A3)}$$

$$L_i^* = (R_2 - R_1)\frac{\sin\gamma_i}{\sin(\pi/2 + \theta_{1,i})} = (R_2 - R_1)\frac{\cos(\alpha + \theta_{1,i})}{\cos\theta_{1,i}} \quad \textbf{(A4)}$$

$$X_i^* = L_i^* \frac{\cos(\theta_{1,i})}{\cos(\alpha - \theta_{1,i})} = (R_2 - R_1)\frac{\cos(\alpha + \theta_{1,i})}{\cos(\alpha - \theta_{1,i})} \quad \textbf{(A5)}$$

The effective area for the i^{th} segment is the area of glass cover through which all reflected radiation is absorbed through the vessel which lied along the line **ec** (Plan of Figure A1). This area is:

$$A_{eff,i} = \pi\left[(R_2 - X_i^*)^2 - R_1^2\right] \quad \textbf{(A6)}$$

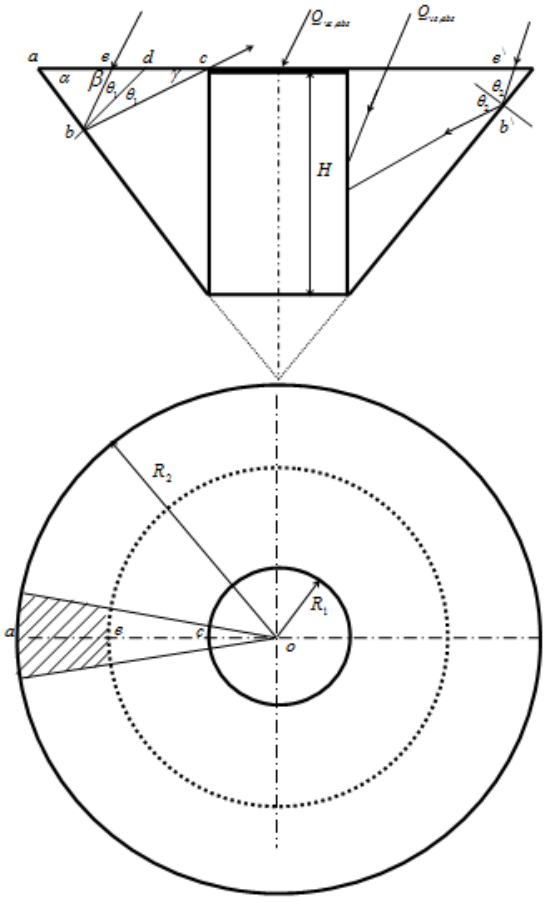

Figure (A1): Different Paths of Solar Radiation through the Glass Cover and Reflected to the Vessel

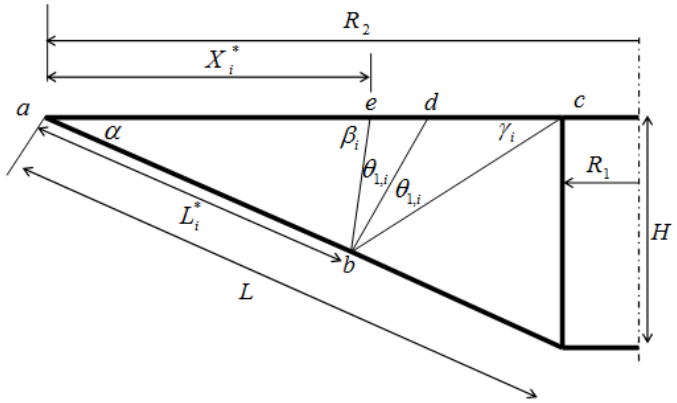

Figure (A2): A Schematic Diagram to Derive the Effective Area of the Glass Cover for i^{th} Segment of the Conical Surface

Special case of (= 45° and at the noon time or normal incidence, i.e. $\theta_{l,\,l} = 45°$, the value of x^*_i is zero by Eq. (A5) and $A_{eff,i} = \pi\ (R_2^2 - R_1^2)$. This means that all incident normal radiation is reflected horizontally and absorbed through the vessel.

Accordingly, the absorbed radiation through the heating vessel included:

a. Reflected radiation from the conical surface. Nearly all reflected radiation on the right half of the conical surface is absorbed through the vessel at all hours, see Figure (A1), and the radiation incident on the CS is depended on its local incidence angle which in tern depended on its local orientation with respect to the south. In the left side of the CS, some of the radiation is reflected and escape to the ambient (represented by the line **are**) while the remain part is absorbed through the vessel. Hence, by dividing the conical surface into N segment, it is possible to calculate the term ($A_{ff,\,l}\ I_i$) for each segment, according to the orientation to the south direction, then, the total absorbed radiation through the vessel is calculated by summing the local area-radiation product as shown in Eq. (A7).

$$Q_{r,abs} = \tau_c\ \rho_{cs}\ \alpha_v \sum_{i=1}^{i=N} A_{eff,i}\ I_i \qquad \textbf{(A7)}$$

Where I_i is the incident radiation on the conical surface and depended on the incidence angle in Eq. (A1).

a. Transmitted radiation through the glass cover and absorbed on the heating vessel surface. The vessel will absorb only the incident radiation on the vertical half facing to the sun while the other half is shaded. Hence, the absorbed radiation through the vessel surface is:

$$Q_{vs,abs} = \tau_c \alpha_v \sum_{i=1}^{i=m} A_{vs,i}\ I_{vs,i} \qquad \textbf{(A8)}$$

Where: (m) is the number of vertical segment of the vessel surface according to the local orientation with the south direction and $I_{vs,i}$ is the solar radiation incident on the i^{th} segment of the vessel.

b. Transmitted radiation through the cover and absorbed through the horizontal cover of the vessel i.e.:

$$Q_{vc,abs} = A_{vc}\ \tau_c\ \alpha_{vc} I_h \quad \textbf{(A9)}$$

Where I_h is the incident radiation on the horizontal surface and calculated by ASHREA model [28].

Finally, the total absorbed radiation through the vessel in Eq. (2) is the summation of absorbed radiations in Eqs (A7-A9).

$$Q_{v,abs} = Q_{r,abs} + Q_{vs,abs} + Q_{vc,abs} \quad \textbf{(A10)}$$

However, the absorbed radiation through the conical surface and glass cover are given in Eqs (A11) and (A12), respectively as:

$$Q_{cs,abs} = \tau_c \alpha_{cs} I_{cs} \quad \textbf{(A11)}$$

$$Q_{c,abs} = \alpha_c I_h \quad \textbf{(A12)}$$

Where: I_{cs} is the incident radiation on the conical surface.